



# Retinal Diseases Detection Of OCT Images Using Ensemble Classification (EC)

Nutralapati Ashok<sup>1\*</sup>, Dr. K. Gangadhara Rao<sup>2</sup>,

## Abstract:

Retinal diseases become more complex for people if they are not identified in the early stages. Diagnosing retinal diseases is time-consuming by using traditional approaches. Early detection of retinal diseases can prevent permanent loss. Optical coherence tomography (OCT) images are grey-scale images that show the back of the human eye which is called the retina. Deep Learning (DL) is most widely used to solve various issues that are more complex. In this paper, an Ensemble classification (EC) is introduced to detect and diagnose retinal diseases by using OCT images. EC is the combination of noise filters that removes the noise from given OCT input images and Convolutional Neural Network (CNN). Preprocessing of OCT images can be done by noise filters. The CNN is the DL model that can classify the OCT images according to the diseases. To improve the performance of EC the edge detection approach is adopted to find the accurate edges of the OCT image. Thus this can help the experts to find the abnormalities present in the OCT input image. This paper focused on classifying the 4 types of diseases as Diabetic Macular Edema (DME), choroidal neovascularization (CNV), Drusen, Age-Related Macular Degeneration (ARMD), and normal case. The pre-trained model VGG-19 is used to train the model with the selected OCT images dataset. The performance of EC is analyzed by using a confusion matrix.

**Keywords:** Ensemble Classification (EC), Deep Learning (DL), Diabetic Macular Edema (DME), choroidal neovascularization (CNV), Drusen, Diabetic Retinopathy (DR).

**DOI Number:** 10.48047/NQ.2022.20.12.NQ77718

**NeuroQuantology 2022;20(12): 3949-3957**

## Introduction

Retinal Diseases are very dangerous if the person not observed in the early stages. Several machine learning methods [1] used hereditary data to anticipate the danger of ARMD with high exactness, showing a region under an Area under the Curve of around 0.8. Studies planning to foresee the movement to cutting edge ARMD coordinating hereditary and clinical information even prompted AUCs of around 0.9, showing that the mix of hereditary and clinical variations are profoundly critical for the expectation of ARMD movement. These models showed achievement in anticipating the long-risk ARMD movement (>5-years). Also, contrasts in populace hereditary qualities may restrict the utilization of current prognostic hereditary tests as most of ARMD hereditary affiliations so far have been concentrated essentially in populaces of European lineage. These discoveries propose the need for extra quality variation concentrates in ARMD reaching out to various populaces. Generic

Retinal diseases pose significant threats to vision and can have a severe impact on a person's quality of life. Diabetic Macular Edema (DME), choroidal neovascularization (CNV), Drusen, and Age-Related Macular Degeneration (ARMD) are among the most common retinal conditions. Detecting these diseases at an early stage is crucial for effective treatment and management. Diabetic Macular Edema (DME) is a complication of diabetes that affects the macula, the central part of the retina responsible for detailed vision. It occurs when fluid accumulates in the macula, causing it to swell and leading to vision loss. Regular eye exams, including comprehensive dilated eye examinations and optical coherence tomography (OCT) scans, are commonly used to detect and monitor DME. Choroidal neovascularization (CNV) involves the growth of abnormal blood vessels beneath the retina,

leading to vision impairment or loss. CNV can

3949

**\*Corresponding Author:**-Nutralapati Ashok

**Address:**<sup>1\*</sup>Research Scholar, Department of CSE, Acharya Nagarjuna University, nutalapati.ashok@gmail.com

<sup>2</sup>Principal, University College of Science, Acharya Nagarjuna University, HOD, Department of CSE, Acharya Nagarjuna University

**Relevant conflicts of interest/financial disclosures:** The authors declare that the research was conducted in the absence of any commercial or financial relationships that could be construed as a potential conflict of interest.



CNV. Drusen are small yellow deposits that accumulate beneath the retina, particularly in individuals with age-related macular degeneration (ARMD). ARMD is a progressive condition that primarily affects older adults and can lead to significant vision loss. Routine eye examinations, including fundus photography and OCT, are utilized to detect drusen and monitor the progression of ARMD. The introduction of advanced imaging technologies has revolutionized the detection and management of retinal diseases. Optical coherence tomography (OCT) is a non-invasive imaging technique that provides high-resolution cross-sectional images of the retina.

It aids in the early detection, diagnosis, and monitoring of retinal diseases by allowing visualization of the retinal layers and detecting subtle abnormalities. Additionally, artificial intelligence (AI) and machine learning algorithms have shown promise in automating the detection and analysis of retinal diseases. These algorithms can analyze large datasets of retinal images, identifying patterns and abnormalities that may be indicative of specific conditions. This technology has the potential to improve the efficiency and accuracy of screening and early diagnosis, enabling timely intervention and treatment.

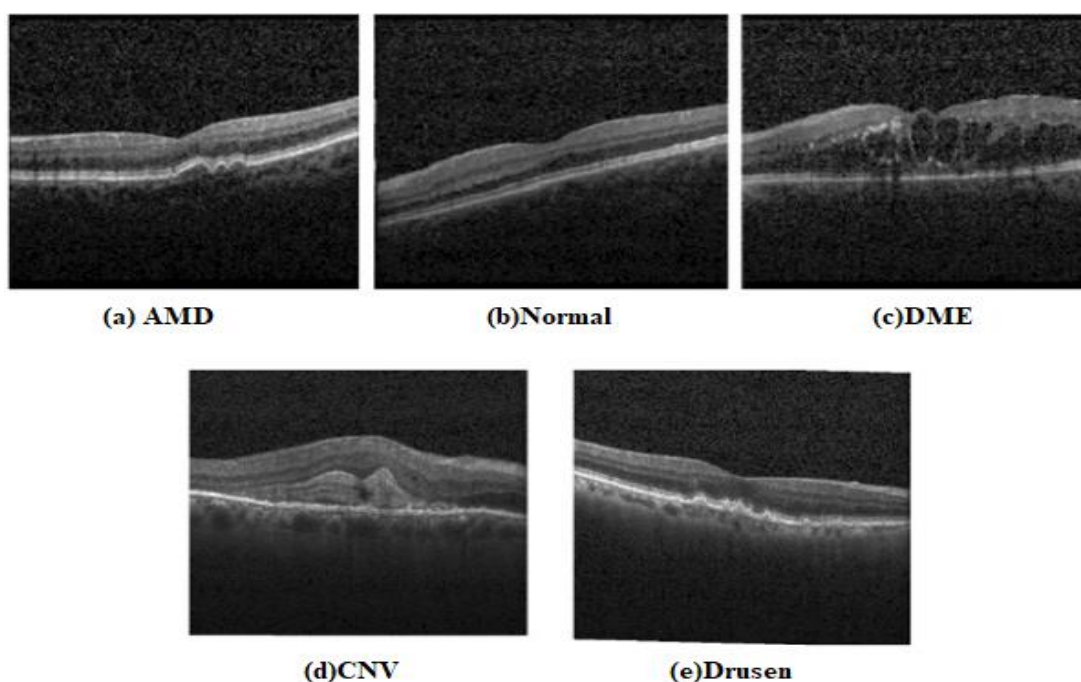


**Figure: 1** (a), (b), (c), (d) and (e) Showing the types of Retinal Diseases (a) AMD (b) Normal (c) DME (d) CNV and (e) Drusen

This paper mainly focused on classifying the OCT images based on their diseases. Every disease has its own properties to find the features of the diseases. The proposed approach consists of multi layers that are used to find the abnormalities in the OCT images. A better pre-trained approach VGG-19 is used to obtain the features to detect specific retinal diseases. The median and Gaussian filters are used to remove the noise from the OCT input image and Laplacian is used find the sharp edges. This helps to increase the disease detection rate.

### Literature Survey

Vali M. [11] introduced the AI-based dynamic

segmentation model that can detect the CNV using OCTA. The CNV is classified into five types of diseases based on the abnormalities. The preprocessing model U-Net network is used to process the input image. In the final step, the segmentation and classification are shown effectively. The proposed model obtained accurate outputs based on the performance. A. Adel et al. [12] proposed automated classification such as CNV, DME, DRUSEN, and specific diseases using OCT images. The automated model combined with two transfer-learning approaches and SVM is used for classification. For performance evaluation, the author used 84k gray-scale images belonging to 4 classes. The accuracy



required for the proposed model is 97.89% compared with the existing model inception V3. Choudhary A et al. [13] proposed an AI-based model combining VGG-19 with transfer learning using OCT images. The proposed model focused on classifying four retinal diseases based on the abnormalities identified in the given samples. The performance of the proposed model is analyzed by using a confusion matrix.

M. Badar et al. [14] introduced automated detection models that detect retinal diseases. The experiments were conducted on 2-D fundus and 3-D OCT images. The authors applied various DL models on different datasets belonging to OCT images. The performance of proposed model was analyzed by using the confusion matrix. H. Fu et al. [15] proposed a new segmentation model that finds the lesions in fundus input images to classify the AMD disease based on the segmented regions. C. Kou et al. [16] proposed the enhanced UNET model for the detection of Microaneurysms (MAs) and exudates (EXs) in the early stages. The proposed model was applied to fundus images collected from online sources. The proposed model extracts the significant features that show the massive impact on results. It developed the residual block that extracts more features, improving the proposed system's performance. Y. Zong et al. [17] proposed an automated segmented model that detects the DR in the early stages. The proposed SLIC approach finds the irregular patches that overcome the issues in

unstructured datasets. Thus the proposed model combined U-net with inception modules and segmentation. The proposed model achieved a better-segmented approach based on the clinical diagnosis. S. Lahmiri [18] proposed the three-stage hybrid classification model that classifies the normal and abnormal retinal images with hemorrhage. The proposed model combines with CNN and SVM to fine-tune the classification results. The evaluation results show the comparison between existing and proposed models.

**Median Filter:**

The median filter is effective for removing salt-and-pepper noise. It replaces each pixel value with the median value of its neighboring pixels. The equation for a median filter is:

$$M(a, b) = \text{median}(P_1, P_2, \dots, P_n) \quad (1)$$

Where:

$M(x, y)$  is the filtered pixel value at position  $(x, y)$ .

$P_1, P_2, \dots, P_n$  are the neighboring pixel values.

To apply the median filter, you slide a window over the image and calculate the median within the window for each pixel.

**Bilateral Filter:**

The bilateral filter preserves edges while reducing noise. It applies a weighted average to neighboring pixels, considering both their spatial distance and pixel intensity differences. The equation for a bilateral filter is:

$$B(a, b) = \left(\frac{1}{W_p}\right) * \sum [i, j \in N] \left( I(a + i, b + j) * S_p(a, b) * S_r(I(a + i, b + j), I(a, b)) \right) \quad (2)$$

Where:

$B(a, b)$  represents the filtered pixel value at position  $(a, b)$ .

$I(a, b)$  is the intensity of the pixel at position  $(a, b)$ .

$S_p(a, b)$  is the spatial weight, which depends on the distance between the neighboring pixel and the central pixel.

$S_r(I(a + i, b + j), I(a, b))$  is the range weight, which depends on the difference in intensity values between the neighboring pixel and the central pixel.

$W_p$  is the normalization factor.

To apply the bilateral filter, you convolve the image with the filter kernel.



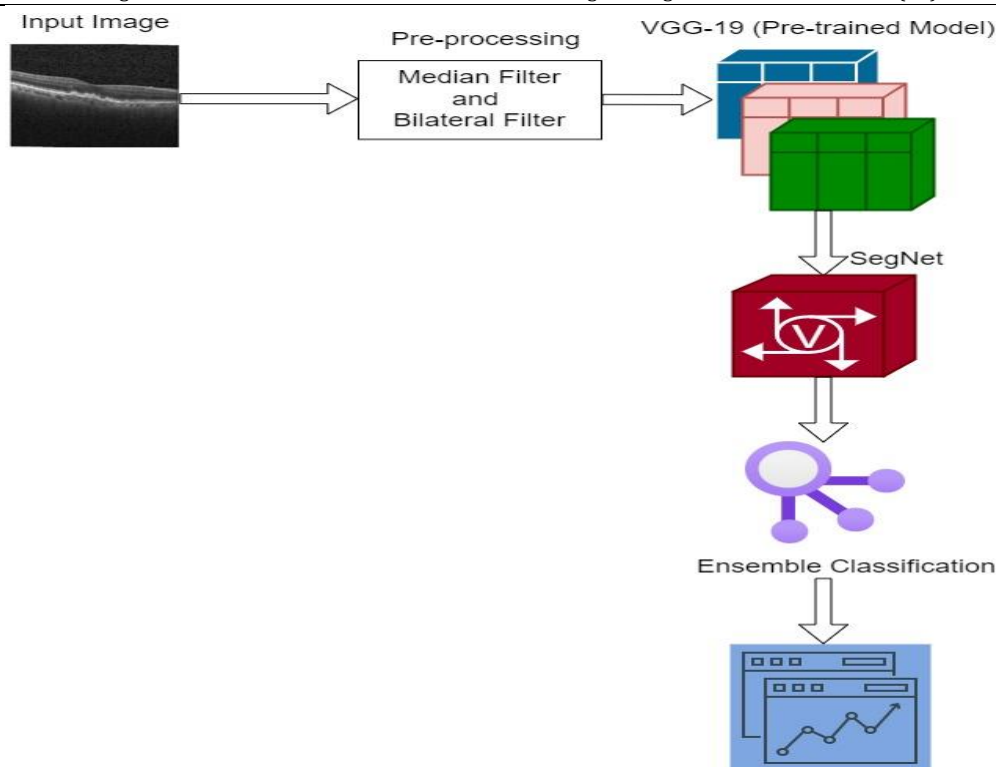


**Figure 2:** Processing steps for Ensemble Classification

### Visual Geometry Group-19 (VGG-19) for Retinal Disease Detection

VGG-19 (Visual Geometry Group 19) is a deep convolutional neural network (CNN) architecture that has gained significant popularity and success in various computer vision tasks, including image classification and object detection. In the context of retinal diseases, VGG-19 has been applied as a powerful tool for automated detection and diagnosis. Retinal diseases encompass a range of conditions that affect the retina, the light-sensitive tissue at the back of the eye. These diseases include diabetic retinopathy, age-related macular degeneration, glaucoma, and retinal detachment, among others. Timely detection and accurate diagnosis of these diseases are crucial for effective treatment and prevention of vision loss. VGG-19 architecture is characterized by its deep structure, consisting of 19 layers, including 16 convolutional layers and 3 fully connected layers. Each convolutional layer employs small filters to extract increasingly complex features from the input image. The use of multiple layers enables the network to learn hierarchical representations, capturing both low-level and high-level features.

To leverage VGG-19 for retinal disease detection, the network is typically trained on a

large dataset of retinal images, labeled with corresponding disease categories. During training, the network learns to recognize patterns and features indicative of different retinal diseases. The process involves adjusting the network's millions of parameters through backpropagation and gradient descent optimization. Once trained, the VGG-19 model can be utilized to classify new, unseen retinal images into different disease categories. By feeding an input image through the network, the model extracts and analyzes various visual features, enabling it to make predictions about the presence or absence of specific retinal diseases.

The advantages of using VGG-19 for retinal disease detection include its ability to learn intricate features from raw image data, its robustness to variations in image quality and lighting conditions, and its generalization capability across different datasets. However, the main limitation of VGG-19 and similar deep learning models is the requirement for a substantial amount of labeled training data, which can be a challenge in medical imaging domains. In conclusion, VGG-19 is a deep convolutional neural network architecture that has shown promise in automated detection and diagnosis of retinal diseases. By leveraging its ability to learn complex visual features, the



model can contribute to early detection, improved patient outcomes, and more efficient healthcare delivery in the field of ophthalmology. VGG-19 consists of 19 layers, including 16 convolutional layers and 3 fully connected layers. Here is a breakdown of the architecture:

**Input layer:** The input to VGG-19 is typically a 224x224 pixel RGB image.

**Convolutional layers:** The network starts with two convolutional layers, each followed by a Rectified Linear Unit (ReLU) activation function and a max-pooling layer for downsampling. These operations help capture low-level features in the image.

**More convolutional layers:** VGG-19 has additional convolutional layers, each with a 3x3 filter size, followed by a ReLU activation and a max-pooling layer. These layers help capture higher-level features and abstract representations.

**Fully connected layers:** After the convolutional layers, the network has three fully connected layers. Each fully connected layer is followed by a ReLU activation, except for the last fully connected layer.

**Output layer:** The final fully connected layer serves as the output layer, typically with a softmax activation function to produce class probabilities for classification tasks.

To adapt VGG-19 for retinal diseases detection, you can remove the last few layers (including the fully connected layers) and replace them with custom layers specific to your task. The modified architecture can be trained on a labeled dataset of retinal images, where the last layer predicts the presence or absence of different retinal diseases.

Keep in mind that fine-tuning VGG-19 for retinal diseases detection may require a significant amount of labeled data and computational resources. Additionally, it's worth exploring other pre-trained models or more specialized architectures designed specifically for retinal disease detection, such as U-Net or RetinaNet, which may yield better results.

### SegNet (Segmentation for Retinal Diseases)

SegNet is an encoder-decoder architecture for pixel-wise segmentation. It uses pooling indices from the encoder stage to upsample feature maps during decoding, helping to retain fine details. SegNet has been utilized for retinal lesion segmentation in various studies. SegNet is a deep learning architecture that was originally developed for semantic segmentation tasks, which involve dividing an image into meaningful regions or segments. While SegNet was not specifically designed for retinal diseases detection, it can be adapted and applied to this task.

Retinal diseases detection typically involves identifying abnormalities or lesions in retinal images that may indicate the presence of various conditions such as diabetic retinopathy, macular degeneration, or retinal detachment. Segmentation plays a crucial role in this process as it helps to isolate and localize these abnormalities within the retinal image. SegNet consists of an encoder-decoder architecture with skip connections. The encoder part extracts high-level features from the input image, while the decoder part reconstructs the segmented output. You would need to modify the last layer of the decoder to match the number of classes in your retinal diseases dataset. It's important to note that while SegNet can be a useful starting point, the success of the model in retinal diseases detection depends on the availability and quality of the labeled dataset, as well as the complexity and variability of the retinal abnormalities you are trying to detect. Additionally, it's always advisable to consult with medical professionals and experts in the field to ensure the accuracy and reliability of any automated system used for medical purposes.

### Ensemble Classification (EC) for Retinal Diseases

Ensemble classification (EC) for retinal diseases using DL refers to a technique where multiple DL models are combined to improve the accuracy and robustness of the classification task for diagnosing retinal diseases. Retinal diseases are conditions that affect the retina, such as DME, CNV, Drusen, ARMD, and normal case. DL is a subfield of artificial intelligence that focuses on training neural networks with multiple layers to extract meaningful features from data. In the context of



retinal disease classification, DL models can be trained on large datasets of retinal images to learn patterns and features that are indicative of specific diseases.

A multiple-layer model with a CNN architecture for the detection of retinal diseases. Please note that the following equations describe the general structure and operations involved in a CNN, but the specific architecture and hyperparameters can vary depending on the implementation and requirements. Let's consider a simplified CNN model with three convolutional layers and two fully connected layers. Each layer performs specific operations, and the equations for those operations are as follows:

### Convolutional Layer:

Inputs: The output from the previous layer or the input image. Let's denote it as  $X$  with dimensions  $[H, W, C]$ , where  $H$  represents the height,  $W$  represents the width, and  $C$  represents the number of input channels.

$$Z_1[i, j, k_1] = \text{sum} \left( \text{sum} \left( \text{sum} (X[p, q, :] * W_1[h, w, :, k_1]) \right) + B_1[k_1] \right) A_1[i, j, k_1] = f(Z_1[i, j, k_1]) \quad (3)$$

### Pooling Layer (Max Pooling):

Input: The output feature map from the previous layer. Let's denote it as  $A_1$ .

$$P_1[i, j, k_1] = \max(A_1[(iS):(iS + FH_2), (jS):(jS + FW_2), k_1]) \quad (4)$$

Here,  $FH_2$  and  $FW_2$  represent the pooling window size, and  $S$  represents the stride.

### Fully Connected Layer:

Input: The flattened output from the previous layer. Let's denote it as  $F_1$  with dimensions  $[N]$ , where  $N$  represents the number of elements.

Weights: The learnable weights for this layer. Let's denote the weights as  $W_2$  with dimensions  $[N, M]$ , where  $M$  represents the number of neurons in this layer.

Biases: The biases for each neuron. Let's denote the biases as  $B_2$  with dimensions  $[M]$ .

Linear Transformation: Apply the matrix multiplication between the input and weights, and add biases to obtain the linear transformation result.

Activation Function: Apply a non-linear activation function to introduce non-linearity.

Weights: The learnable filters for the convolution operation. Let's denote the weights for this layer as  $W_1$  with dimensions  $[FH_1, FW_1, C, K_1]$ , where  $FH_1$  represents the filter height,  $FW_1$  represents the filter width,  $C$  represents the number of input channels, and  $K_1$  represents the number of filters.

Biases: The biases for each filter. Let's denote the biases for this layer as  $B_1$  with dimensions  $[K_1]$ .

Convolution Operation: Apply the convolution operation using the weights and biases to obtain the output feature map  $Z_1$ .

Activation Function: Apply a non-linear activation function, such as ReLU (Rectified Linear Unit), to introduce non-linearity. Let's denote the activation function as  $f()$ .

Output: The output feature map after the activation function is applied, denoted as  $A_1$ .

The equations for the convolution operation and activation function are as follows:

Pooling Operation: Apply the max pooling operation to reduce the spatial dimensions and extract the most important features.

Output: The down sampled feature map, denoted as  $P_1$ .

The equations for max pooling are as follows:

Output: The output of the fully connected layer, denoted as  $A_2$ .

The equations for the fully connected layer are as follows:

$$L_2 = F_1 @ W_2 + B_2 \quad (5)$$
$$A_2 = f(L_2) \quad (6)$$

### Output Layer:

Input: The output from the previous layer. Let's denote it as  $A_2$ .

### Experimental Results

The above algorithm is implemented through python programming language for the given input OCT images. The dataset is collected from the kaggle website and this contains 5000 images with 5 categories. The source is <https://www.kaggle.com/datasets/paultimoth>



ymooney/kermany2018. This dataset contains 5000 training and 5000 testing. This is labeled dataset contains CNV, DRUSEN, DME, AMD and normal 1000 each. The system hardware 8 GB RAM is required for the processing of large datasets.

**Performance Metrics**

The confusion matrix is used to analyze the classification algorithm performance. Measuring the performance with a confusion matrix gives a better for find the accurate errors. It is also used to solve several classification issues. This can be applied for classification of binary issues and also for multiclass classification issues. The count values are based on various attributes such as

**TP:** In this the actual value of true (disease present) and predicted value is true (disease present).

**TN:** The actual value is true (disease present) and predicted value is false (No disease).

**FP:** The actual value is false (No disease) and predicted value is true (disease present).

**FN:** The actual value is false (No disease) and predicted value is false (No disease).

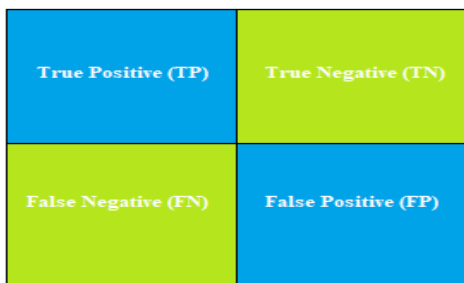


**Figure 3:** Confusion Matrix

**Sensitivity (S<sub>n</sub>):** Sensitivity, recall, or the TP rate (TPR) is the fraction of positive values out of the total actual positive instances (i.e., the

proportion of actual positive cases that are correctly identified):

$$S_n = \frac{TP}{TP + FN}$$

**Specificity (S<sub>p</sub>):** Specificity gives the fraction of negative values out of the total actual negative instances. In other words, it is the proportion of actual negative cases that are correctly identified. The FP rate is given by (1 - specificity):

$$S_p = \frac{TN}{TN + FP}$$

**Precision (P):** Precision or the positive predictive value, is the fraction of positive values out of the total predicted positive instances. In other words, precision is the proportion of positive values that were correctly identified:

$$P = \frac{TP}{TP + FP}$$

**Accuracy (Acc):** Accuracy shows the total number of prediction that is correct. Actual and predicted values are correct. It is represented with below formula.

$$Acc = \frac{TP + TN}{TP + FP + TN + FN}$$

**F1-Score (F1S):** The F1-score combines the precision and recall of a classifier into a single metric by taking their harmonic mean.

$$F1S = 2 * \frac{P * S_n}{P + S_n}$$

**Table 1:** Confusion Matrix count values

Count Values	CNN	RESNET	EC
TP	2378	2675	2879
TN	2213	2087	1856
FP	245	125	165
FN	114	64	98

**Table 2** Shows the Performance of Existing and Proposed Algorithms for detection of CNV

	CNN	ResNet	EC
<b>Sensitivity (SE)</b>	77.22	86.76	98.98
<b>Specificity (SP)</b>	81.54	85.76	98.56
<b>Precision (PE)</b>	80.65	85.43	98.34
<b>Accuracy (ACC)</b>	81.66	87.52	97.76
<b>F1-Score</b>	82.12	87.53	97.58



**Table 3** Shows the Performance of Existing and Proposed Algorithms for detection of DME

	CNN	ResNet	EC
<b>Sensitivity (SE)</b>	78.32	86.78	98.96
<b>Specificity (SP)</b>	81.34	87.34	98.12
<b>Precision (PE)</b>	82.34	88.43	98.44
<b>Accuracy (ACC)</b>	82.45	87.12	98.12
<b>F1-Score</b>	83.12	88.43	98.56

**Table 4** Shows the Performance of Existing and Proposed Algorithms for detection of Drusen

	CNN	ResNet	EC
<b>Sensitivity (SE)</b>	79.32	87.64	98.89
<b>Specificity (SP)</b>	82.34	87.87	97.12
<b>Precision (PE)</b>	82.34	88.53	97.34
<b>Accuracy (ACC)</b>	83.45	86.12	98.12
<b>F1-Score</b>	84.12	87.43	98.56

**Table 5** Shows the Performance of Existing and Proposed Algorithms for detection of AMD

	CNN	ResNet	EC
<b>Sensitivity (SE)</b>	78.12	85.34	98.56
<b>Specificity (SP)</b>	80.34	86.34	97.34
<b>Precision (PE)</b>	81.34	87.43	99.34
<b>Accuracy (ACC)</b>	82.45	86.12	99.45
<b>F1-Score</b>	82.12	86.43	98.56

**Table 6** Shows the Performance of Existing and Proposed Algorithms for detection of Normal

	CNN	ResNet	EC
<b>Sensitivity (SE)</b>	71.12	84.34	99.56
<b>Specificity (SP)</b>	81.34	87.12	98.34
<b>Precision (PE)</b>	82.34	87.98	99.67
<b>Accuracy (ACC)</b>	83.45	85.89	99.78
<b>F1-Score</b>	84.12	87.09	99.89

**Table 7** Shows the Performance of Existing and Proposed Algorithms for detection of Overall performances

	CNN	ResNet	EC
<b>Sensitivity (SE)</b>	73.32	83.34	99.23
<b>Specificity (SP)</b>	81.64	88.12	98.34
<b>Precision (PE)</b>	82.74	88.98	99.45
<b>Accuracy (ACC)</b>	84.85	89.89	99.76
<b>F1-Score</b>	84.78	88.19	99.67

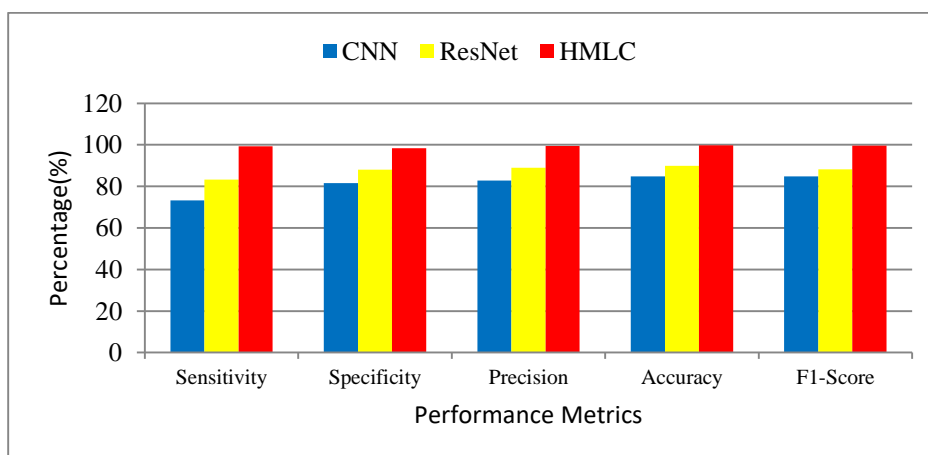


**Figure 4:** Performance graph for CNN, RESNET and EC





## Conclusion

This paper mainly focused on diagnosing and detecting retinal diseases by using hybrid multi-layered classification (EC). The EC is one of the significant approaches that can classify diseases based on their properties of the diseases. To remove the uncertainty from the input OCT images the salt and pepper noise filter is used to sharpen the input image. The Edge detection approach is used to find the accurate edges of the OCT images to find the missing abnormalities present in the input images. The pre-trained model VGG19 obtained the features from the given training dataset and helps the proposed model for the classification of retinal diseases. Figure 4 shows the performance comparisons between traditional and proposed models achieved the better performance compared with tradition approaches based on Sensitivity (SE) is 99.23, Specificity (SP) is 98.34, Precision (PE) is 99.45, Accuracy (ACC) is 99.76 and F1-Score is 99.67. Hence, the EC classified and detected the four types of retinal diseases with better disease detection rate.

## References

1. Md Shakib Khan, Nafisa Tafshir, Kazi Nabiul Alam, Abdur Rab Dhruba, Mohammad Monirujjaman Khan, Amani Abdulrahman Albraikan, Faris A. Almalki, "Deep Learning for Ocular Disease Recognition: An Inner-Class Balance", *Computational Intelligence and Neuroscience*, vol. 2022, Article ID 5007111, 12 pages, 2022. <https://doi.org/10.1155/2022/5007111>.
2. M. Z. Atwany, A. H. Sahyoun and M. Yaqub, "Deep Learning Techniques for Diabetic Retinopathy Classification: A Survey," in *IEEE Access*, vol. 10, pp. 28642-28655, 2022, doi: 10.1109/ACCESS.2022.3157632.
3. P. Vora and S. Shrestha, "Detecting diabetic retinopathy using embedded computer vision," *Appl. Sci.*, vol. 10, no. 20, p. 7274, Oct. 2020.
4. Z. J. Hussein and E. H. Al Saadi, "Recent Developments Used for Early Detection of Diabetic Macular Edema by Retinal Images: A survey," 2022 Iraqi International Conference on Communication and Information Technologies (IICCIT), Basrah, Iraq, 2022, pp. 335-341, doi: 10.1109/IICCIT55816.2022.10010431.
5. Z. Li et al., "Automated detection of retinal exudates and drusen in ultra-widefield fundus images based on deep learning", *Eye*, pp. 1-6, January 2021.
6. L. Ju et al., "Improving Medical Images Classification With Label Noise Using Dual-Uncertainty Estimation," in *IEEE Transactions on Medical Imaging*, vol. 41, no. 6, pp. 1533-1546, June 2022, doi: 10.1109/TMI.2022.3141425.
7. J. Huang, L. Qu, R. Jia and B. Zhao, "O2U-Net: A simple noisy label detection approach for deep neural networks", *Proc. IEEE Int. Conf. Comput. Vis.*, pp. 3326-3334, Oct. 2019.
8. X. He, Y. Deng, L. Fang and Q. Peng, "Multi-Modal Retinal Image Classification With Modality-Specific Attention Network," in *IEEE Transactions on Medical Imaging*, vol. 40, no. 6, pp. 1591-1602, June 2021, doi: 10.1109/TMI.2021.3059956.
9. X. Liu, J. Cao, S. Wang, Y. Zhang and M. Wang, "Confidence-Guided Topology-Preserving Layer Segmentation for Optical Coherence Tomography Images With Focus-Column Module," in *IEEE Transactions on Instrumentation and Measurement*, vol. 70, pp. 1-12, 2021, Art no. 5005612, doi: 10.1109/TIM.2020.3047430.
10. Y. Xie, J. Zhang, H. Lu, C. Shen and Y. Xia, "SESV: Accurate Medical Image Segmentation by Predicting and Correcting Errors," in *IEEE Transactions on Medical Imaging*, vol. 40, no. 1, pp. 286-296, Jan. 2021, doi: 10.1109/TMI.2020.3025308.
11. Vali, M.; Nazari, B.; Sadri, S.; Pour, E.K.; Riazi-Esfahani, H.; Faghihi, H.; Ebrahimiadib, N.; Azizkhani, M.; Innes, W.; Steel, D.H.; Hurlbert, A.; Read, J.C.A.; Kafieh, R. CNV-Net: Segmentation, Classification and Activity Score Measurement of Choroidal Neovascularization (CNV) Using Optical Coherence Tomography Angiography (OCTA). *Diagnostics* 2023, 13, 1309. <https://doi.org/10.3390/diagnostics13071309>.
12. A. Adel, M. M. Soliman, N. E. M. Khalifa and K. Mostafa, "Automatic Classification of Retinal Eye Diseases from Optical Coherence Tomography using Transfer Learning," 2020 16th International Computer Engineering Conference (ICENCO), Cairo, Egypt, 2020, pp. 37-42, doi: 10.1109/ICENCO49778.2020.9357324.
13. Choudhary A, Ahlawat S, Urooj S, Pathak N, Lay-Ekuakille A, Sharma N. A Deep Learning-Based Framework for Retinal Disease Classification. *Healthcare (Basel)*. 2023 Jan 10;11(2):212. doi: 10.3390/healthcare11020212. PMID: 36673578; PMCID: PMC9859538.
14. M. Badar, M. Haris, and A. Fatima, "Application of deep learning for retinal image analysis: A review," *Comput. Sci. Rev.*, vol. 35, Feb. 2020, Art. no. 100203.
15. H. Fu, F. Li, J. I. Orlando, H. Bogunovic, X. Sun, J. Liao, Y. Xu, S. Zhang, and X. Zhang, "Adam: Automatic detection challenge on age-related macular degeneration [data set]," in *Proc. IEEE DataPort*, 2020.
16. C. Kou, W. Li, Z. Yu, and L. Yuan, "An enhanced residual U-Net for microaneurysms and exudates segmentation in fundus images," *IEEE Access*, vol. 8, pp. 185514-185525, 2020.
17. Y. Zong, J. Chen, L. Yang, S. Tao, C. Aoma, J. Zhao, and S. Wang, "Unet based method for automatic hard exudates segmentation in fundus images using inception module and residual connection," *IEEE Access*, vol. 8, pp. 167225-167235, 2020.
18. S. Lahmiri, "Hybrid deep learning convolutional neural networks and optimal nonlinear support vector machine to detect presence of hemorrhage in retina," *Biomed. Signal Process. Control*, vol. 60, Jul. 2020.

